Connecting an Offshore Dry Air Stratospheric Intrusion with the Outbreak of Soberanes Fire 2016

JODIE CLARK[a] AND SEN CHIAO[b]

[a] *San Jose State University, San Jose, California*
[b] *Howard University, Washington, D.C.*

(Manuscript received 6 March 2023, in final form 29 November 2023, accepted 3 December 2023)

ABSTRACT: This study investigates the connection between the arrival of dry stratospheric air and the Soberanes Fire (2016). The Hybrid Single-Particle Lagrangian Integrated Trajectory model (HYSPLIT) and Goddard Earth Observing System Forward Processing model (GEOS-FP) are used for back-trajectories and offshore deep stratospheric intrusion in conjunction with the ignition and outbreak of the fire. The back-trajectory analysis indicates that most air reaching the vertical column was critically dry, exhibiting relative humidity values below 10%. As the fire ignited, dry air arrived from due west at heights of 1–3 km about 24 h prior. During the overnight fire growth, dry air arrived from the northwest to north-northwest at heights of 3.5–5.5 km 48–72 h prior. The synoptic and GEOS-FP analyses demonstrate offshore mid-to-low stratospheric intrusion. On 21 July 2016, an enclosed upper-level low approached the California–Oregon border along the northwesterly subtropical jet stream hours before the fire outbreak. The GEOS-FP results of potential vorticity, specific humidity, and ozone along the back-trajectories to the west and northwest of the fire suggest a stratospheric intrusion event into the mid-to-low troposphere at the back-trajectory start points, and vertical velocity indicates sinking motion. The specific humidity analyzed at the arrival time shows the transport of the abnormally dry air to the Soberanes Fire. Results suggest a connection between dry stratospheric air transported to the Soberanes Fire at ignition and overnight accelerated growth, supported by a dark bank in satellite water vapor imagery. The prediction of low-level transport of dry stratospheric air to the coastal communities could help to predict the occurrence of wildfire outbreaks, or periods of accelerated fire growth.

KEYWORDS: Dry intrusions; Potential vorticity; Wildfires; Ozone

1. Introduction

A well-known four critical weather elements common to wildfire exhibiting extreme behavior include unusually low relative humidity (RH), strong surface winds, unstable air, and drought conditions (Werth et al. 2011). Of these four elements, low RH values must be present with either strong surface winds or unstable air. Drought and related vegetation dryness are essential requirements for wildfire ignition and development. Wildfire frequency and strength have increased in California in recent droughts years (Spracklen et al. 2009; Boegelsack et al. 2018; Williams et al. 2019). A 30-yr study of wildfires in the northwestern United States found that 80% of very large wildfires occurred in August (44.3%) and July (37.0%), including extremely large wildfires that occurred in 6 of the 20 states including California (Zhong et al. 2020).

Nevertheless, an often-overlooked important factor is dry air transported from the upper atmosphere. Zimet et al. (2007) showed that a well-developed dry air intrusion extended to nearly the 750-hPa level far downstream from an upper-frontal zone supplying the fire environment with dry air that originated in the upper-troposphere/lower stratosphere. Mills (2008) summarized an abrupt surface drying (i.e., lowering of the surface humidity) and its relationship with midtropospheric dry air, and the synoptic dynamics that allowed the ignition of wildfires in South Australia. While we often look at stratospheric intrusions regarding air pollution and ozone transport, another important aspect of the events is the link between a deep offshore stratospheric intrusion and wildfires. Schoeffler (2009) summarized that dry intrusions (i.e., dry slots) manifest themselves as clearly visible dark bands in the satellite water vapor imagery. These dry slots usually result in abrupt surface drying and strong, gusty winds often radically influencing wildland fire behavior and hence fire growth. A similar fire weather condition with the passage of negatively tilted upper-tropospheric troughs, which lead to a descent into the atmospheric boundary layer of dry, high-momentum air also occurred in Tasmania, Australia (Fox-Hughes 2015). Furthermore, Langford et al. (2015) suggest that the northerly winds and the extremely dry air descending to the surface on the western flank of the trough associated with a deep stratospheric intrusion (SI) brought conditions for the explosive May 2013 Springs Fire in Camilla, California. The important analysis of the 2017 northern California wildfires by Mass and Ovens (2019) synoptic evaluation presents a case that one could interpret as that of a powerful SI event.

Cho et al. (2001) showed that with the presence of a dry, ozone-rich SI with high static stability, a convective pollution plume rising from the ground could be capped and flattened. Using satellite measurements Georgiev et al. (2022) concluded that the depth of dry stratospheric intrusions, the associated synoptic evolution, and the enhanced low-level O_3

Clark's current affiliation: DSG Solutions, LLC, Shoreline, Washington.

Corresponding author: Sen Chiao, sen.chiao@howard.edu

DOI: 10.1175/JAMC-D-23-0043.1

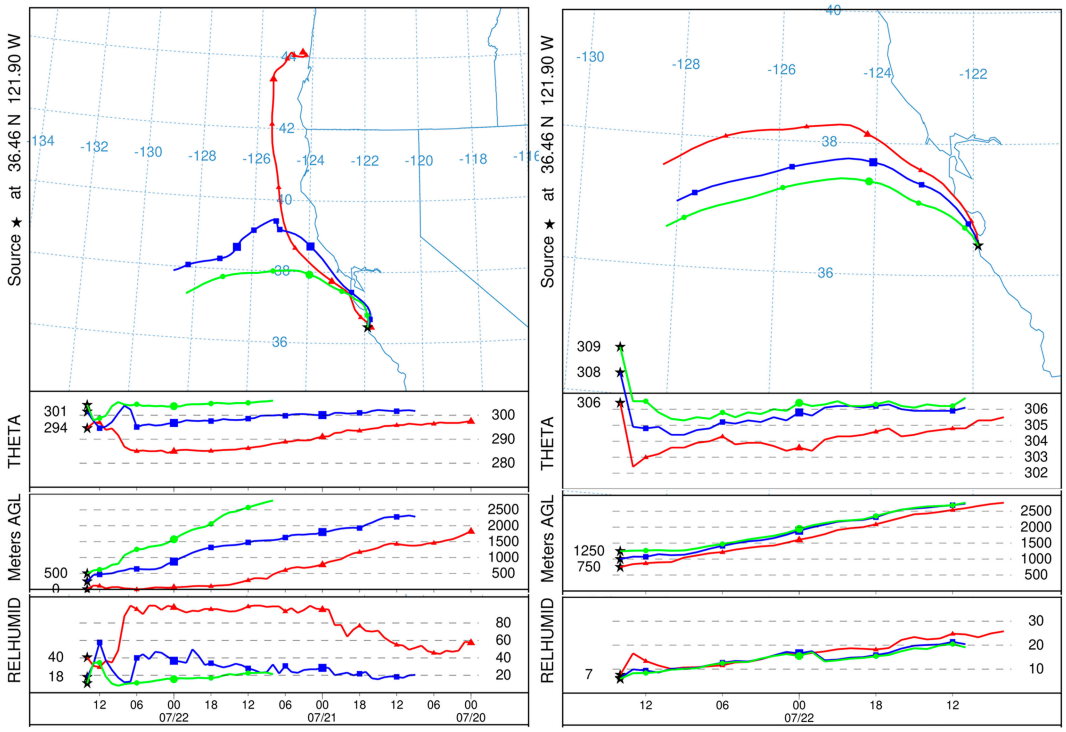

FIG. 1. NOAA HYSPLIT model back-trajectories ending at 1400 UTC 22 Jul 2016, using HRRR meteorological data, displaying potential temperature, meters AGL, and RH along the trajectory.

concentrations were caused by vertical transport of stratospheric air and/or related to biomass burning emissions. Apparently, observations of plume dispersion can second the event of daytime near-surface intrusions.

Prior studies have used potential vorticity (PV) and layered structures in ozone profiles to identify stratospheric air masses (e.g., Danielsen et al. 1987; Oltmans et al. 2010; Roelofs et al. 2003; Škerlak et al. 2014; Clark and Chiao 2019). A value of 1 potential vorticity unit (PVU; 1 PVU = 10^{-6} K kg^{-1} m^2 s^{-1}) is best suited to investigate the deep descent of dry stratospheric air transporting O_3 into the troposphere, with the possibility of even lower values showing the elongated tongues of the intrusions into lower levels (Cox et al. 1997; Trickl et al. 2014). Dry air within the region of high PV would indicate the presence of air that exhibits stratospheric conditions, carrying abundant O_3 concentrations.

On the other hand, it is also well known that in the tropics, convection or rising motion is present ahead of the SI event in the direction of travel, with strong sinking motion and dry air behind the PV-intrusion (Funatsu and Waugh 2008). The concept could help identify SIs in the midlatitudes, but potentially harder to identify forward motion due to the larger amplitude waves along the polar jet stream and even the subtropical jet stream.

This study aims to investigate the connection between the coastal Soberanes Fire (2016) outbreak and the arrival of near-surface dry stratospheric air with an offshore deep SI event. The Soberanes Fire of Monterey County, California, ignited on 22 July 2016, in the morning hours around 0848 Pacific daylight time (PDT) (1548 UTC) from an illegal campfire. It remained active for nearly 3 months, burning 132 127 acres (1 acre ≈ 0.4 ha) at the central Coastal Range and into the Los Padres National Forest (Potter 2016). A state of emergency in Monterey County was declared on 26 July as the fire rapidly grew by 5000 acres and entered federal parks. The fire grew by similar acreage overnight from 3 August into 4 August. As defined in Potter (2016), during the first stage of the Soberanes Fire, it grew to ~45% of its total acreage in just 17 days by 7 August. The period is denoted in Potter (2016) as extremely dry with large fire spread and will be the period of focus for this study. The Soberanes Fire burned for 10 weeks and was finally 100% contained on 11 October 2016.

This research is categorized into several objectives that aim to analyze that a deep offshore SI brought extreme fire weather conditions to the coastal mountains where the Soberanes Fire ignited, indicating a connection between the events. The first objective is to demonstrate that a deep offshore SI occurred on 21 July 2016. The second objective is to show the transport of air from the region of stratospheric injection to the coastal California Soberanes Fire outbreak that occurred on the morning of 22 July 2016. The third objective is to evaluate the period from 21 July to 7 August for temporal and spatial anomalies that would indicate the strength/presence of a deep SI and the presence of extreme fire weather conditions. The last objective is to present the case that the connection between summer SI events and fire weather needs deeper investigation. A successful analysis would prove to be a helpful forecasting tool for the community and will

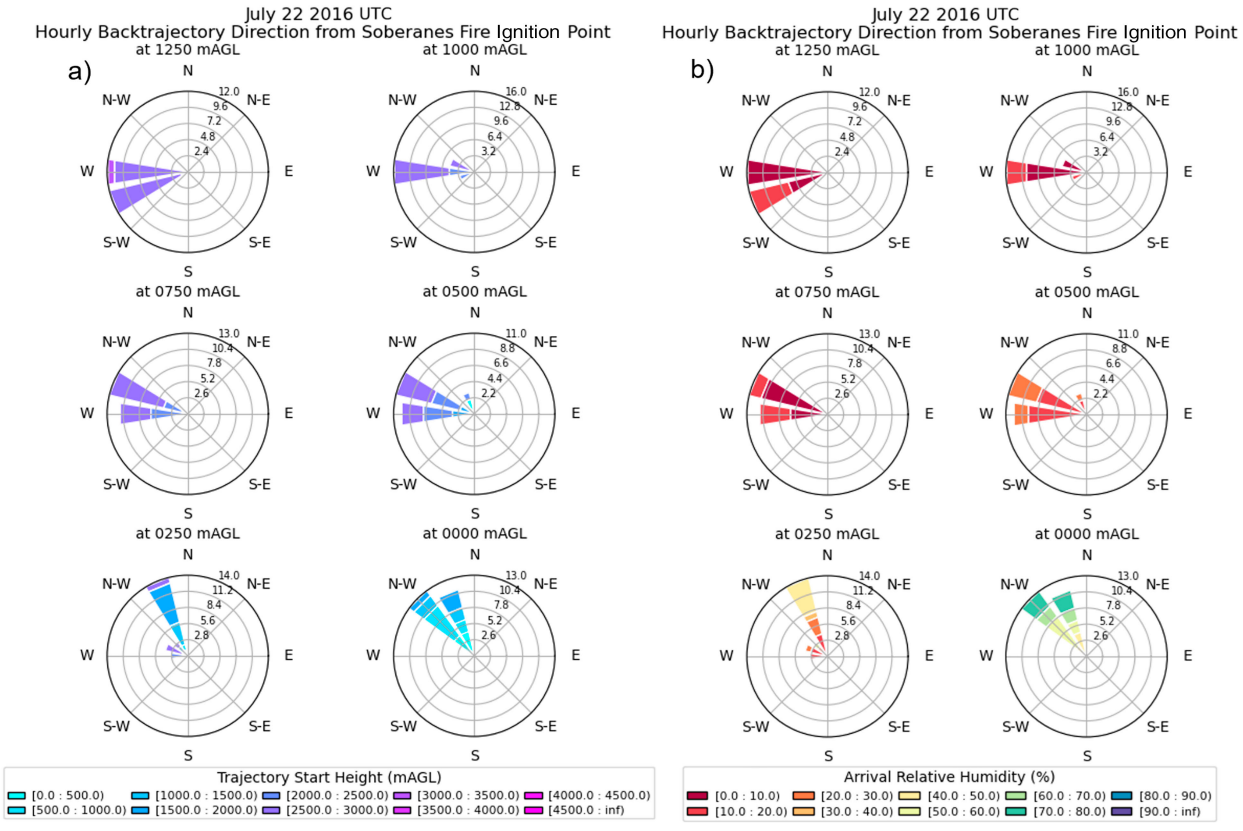

FIG. 2. Hourly back-trajectory direction from the Soberanes Fire ignition point for each starting height on 22 Jul 2016 (PDT; UTC − 7 h) for (a) trajectory start height and (b) arrival relative humidity.

contribute to our knowledge of the connection between SI events and fire outbreaks/growth.

Data and analysis methods are in section 2. The results of Hybrid Single-Particle Lagrangian Integrated Trajectory (HYSPLIT) analysis, along with analysis of synoptic and mesoscale patterns associated with the 2016 Soberanes Fire characteristics, including measured observations, are discussed in section 3. In section 4, the conclusions of this study are provided.

2. Data and analysis methods

a. *HYSPLIT model*

The 3-km High-Resolution Rapid Refresh (HRRR) model output is employed for the NOAA/Air Resources Laboratory (ARL) HYSPLIT (Stein et al. 2015) back-trajectories to evaluate the upper air entering the coastal California Soberanes Fire region. The HRRR is a NOAA real-time 3-km-resolution, hourly updated, cloud-resolving, convection-allowing atmospheric model, initialized by 3-km grids with 3-km radar assimilation. Radar data are assimilated in the HRRR every 15 min over a 1-h period, adding further detail to that provided by the hourly data assimilation from the 13-km radar-enhanced Rapid Refresh. More information on the HRRR can be obtained from NOAA/ESRL.

The back-trajectory end location is set to the ignition latitude and longitude for the fire (36.459 94°N, 121.899 38°W). The back-trajectory model runs were set to a duration period of 72 h for six elevations aloft between 0 and 1250 m AGL in increments of 250 m. This was performed hourly for a 24-h period starting at 0000 UTC 22 July 2016. For each hour and level, the back-trajectories were evaluated for the starting location and time, the arrival or endpoint RH, and, if relatively constant, the potential temperature θ and the directionality of the air entering the region of the Soberanes Fire. Only relatively constant potential temperature was considered for the back-trajectory frequency starting location because the air would remain stratospheric in nature. From this back-trajectory analysis, two important time stamps were identified for the rest of the analysis method; first, the back-trajectory arrival time and Soberanes Fire outbreak that occurred at 1500 UTC 22 July, and second, the back-trajectory start time at 1200 UTC 21 July.

b. *GEOS-FP model*

Multiple Goddard Earth Observing System Forward Processing (GEOS-FP) data variables are evaluated to define the occurrence of a SI event. The version of 5.13.1 GEOS-FP with horizontal resolution 0.25° latitude × 0.3125° longitude resolution was used. More detailed information about the GEOS model system is available at the NASA Global

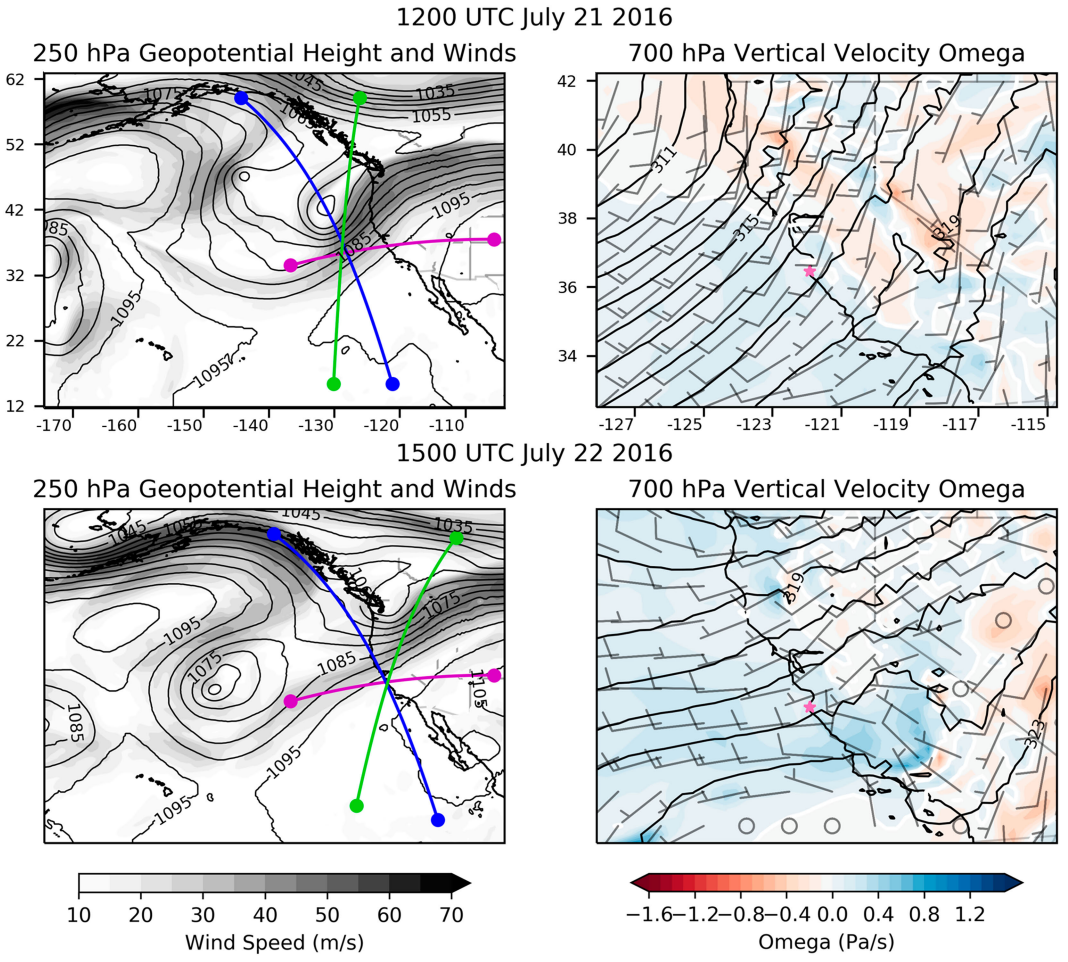

FIG. 3. GEOS-FP results of (left) 250-hPa geopotential height (contours) and wind speed (shading) and (right) 700-hPa geopotential height (contours), vertical velocity (omega; color shading), and wind speed and direction (barbs and lines), valid at (top) 1200 UTC 21 and (bottom) 1500 UTC 22 Jul 2016. Blue, green, and purple lines represent cross sections; the pink star represents the Soberanes Fire ignition point.

Modeling and Assimilation Office (GMAO). With this approach, a deep offshore SI can be identified using the region and time of interest from the back-trajectory frequency analysis. The 250-hPa geopotential heights and winds for the eastern Pacific/western North American region are evaluated to understand the synoptic conditions in association with jet stream placement around the high and low pressure centers. To further evaluate mesoscale properties for the California region and to identify areas of strong sinking motion into the lower troposphere, vertical motion omega and wind speed and direction at 700 hPa are evaluated at the back-trajectory start and arrival times that also correspond to the back-trajectory starting height.

To better gauge the scope of the deep offshore intrusion and the continued transport into the lowest kilometer above ground at the western coastal mountains, multiple-vertical-cross-section analysis is performed. The west–east cross section is along the back-trajectory path from start to end; the northwest–southeast cross section and the southwest–northeast cross section are first centered at the back-trajectory frequency starting location, and second for the arrival location, also known as the Soberanes Fire ignition point. The cross-section analysis evaluates modeled PV values ranging between 0.8 and 5.0 PVU, specific humidity (SH) values between 0.015 and 5.0 g kg^{-1}, and ozone (O_3) values to identify the initial wave break of the tropopause, the extended tongue through the troposphere, and dispersion of stratospheric air into the lower troposphere. The O_3 and SH also are used as a tracer of the continued transport of the dry stratospheric air to the lowest 1.25 km above the Soberanes Fire. Vertical velocity (omega) points to the important regions of sinking motion associated with the initial deep offshore SI, the continued descent of the dry stratospheric air mass to the coastal Soberanes Fire outbreak site, and to identify low-level mixing or instability near the wildfire. When observing PV structure in association with O_3 in the lower troposphere and near the surface, the SH values and the omega are essential to distinguish the placement of higher PV values caused by diabatic heating below 3 km.

An evaluation of period averages and anomalies is conducted to strengthen the argument of the continued stratospheric transport

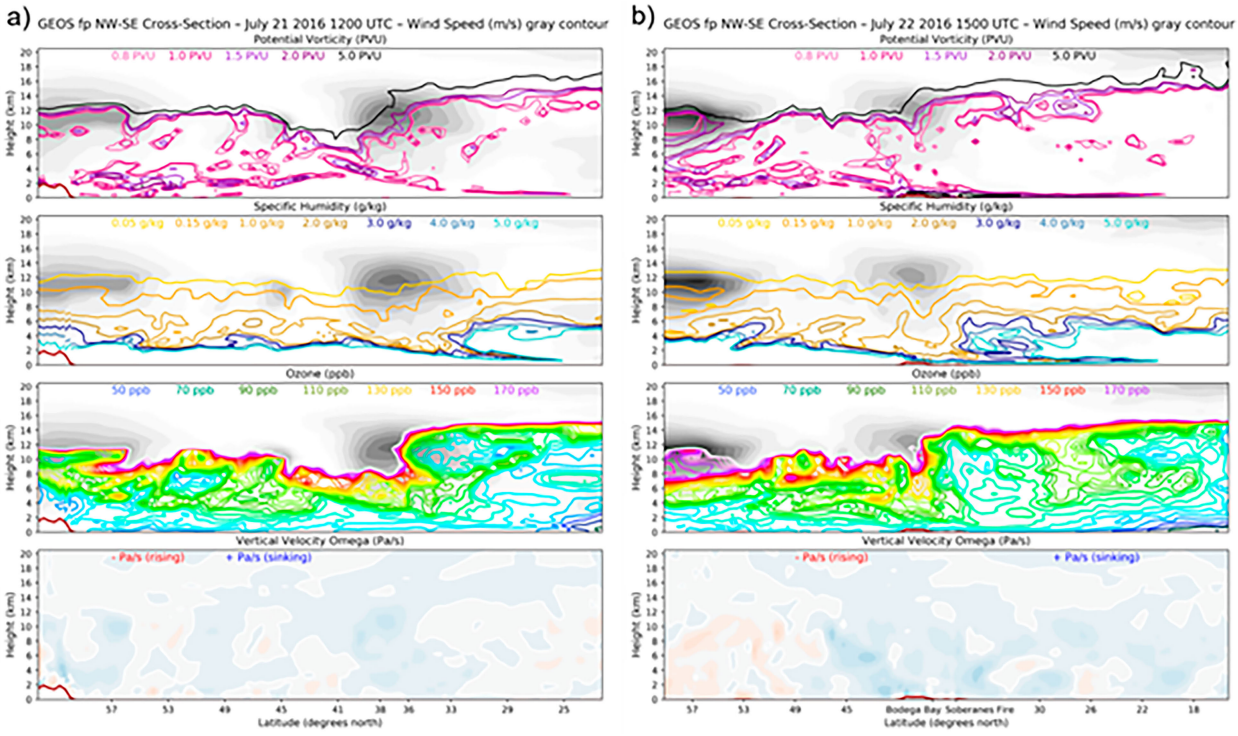

FIG. 4. Northwest–southeast cross sections (blue line in Fig. 3), showing GEOS-FP potential vorticity, specific humidity, ozone, and vertical velocity omega at (a) 1200 UTC 21 and (b) 1500 UTC 22 Jul 2016. The grayscale wind speed mimics that of Fig. 3.

and the presence of extreme fire weather conditions. The period averages are calculated from 0000 UTC 21 July through stage 1 of the Soberanes Fire, which was described in Potter (2016) (i.e., 0000 UTC 21 July–2100 UTC 7 August), and the anomalies evaluated are for the back-trajectory start on 1200 UTC 21 July and the Soberanes Fire outbreak of 1500 UTC 22 July. These cover the geopotential heights and wind speed for the eastern Pacific/western North American region and are performed at 250, 500, and 700 hPa. The sea level pressure is also evaluated. The average planetary boundary layer (PBL) heights and the average surface SH values at 1430 UTC are calculated across the period over a local fire region, and anomalies for the Soberanes Fire outbreak at 1430 UTC 22 July are evaluated.

3. Results and discussion

a. HYSPLIT back-trajectory analysis

Over the 24-h observation period, each of the HYSPLT model runs for 750–1250 m AGL demonstrated dry air entering from the west, descending from 2 to 3 km down a relatively constant isentrope. Results suggested no significant changes to the stratospheric air mass. Leading up to and at the time of the Soberanes Fire outbreak, the air entering the region was very dry, especially at 500–1250 m AGL, where RH values reached critical levels as low as 6%. The surface arrival RH decreases with time to a minimum of 40% just before the Soberanes Fire outbreak at 1300–1400 UTC; shown in Fig. 1 for 1400 UTC 22 July 2016, about 1 h prior to ignition.

The wind-rose analyses, as shown in Fig. 2, summarized the 24-h back-trajectory results for starting direction, start height, and ending RH percentages for each of the six end heights. As trajectory end height increases, the winds veer with the height from the north-northwest to the west-southwest and humidity drops from 60% to below 10% within 1250 m. The driest air entered from the west at an elevation between 750 and 1250 m. At 500 m AGL, RH values were no greater than 30%, and at 250 m AGL, RH values ranged between as low as 10% and up to 50%. Of most importance, air that reached the lowest 1.25 km above the Soberanes Fire with less than 30% RH entered from the west near 128°W and between 36° and 38°N with a starting elevation between 2 and 3.5 km; now defined as the start point. It appears that these trajectory paths also followed a relatively constant isentrope to the arrival height elevated above the Soberanes Fire ignition point. It can be concluded that much of the air entering the Soberanes Fire region exhibited qualities of stratospheric air: very dry air descending quickly (~500 m every 3 h) from greater heights down a constant isentrope within a short time.

b. Synoptic/mesoscale analysis

The 250-hPa geopotential heights and winds 27 h prior to the Soberanes Fire outbreak indicate an area of high pressure in the western Gulf of Alaska and a deep, broad trough over

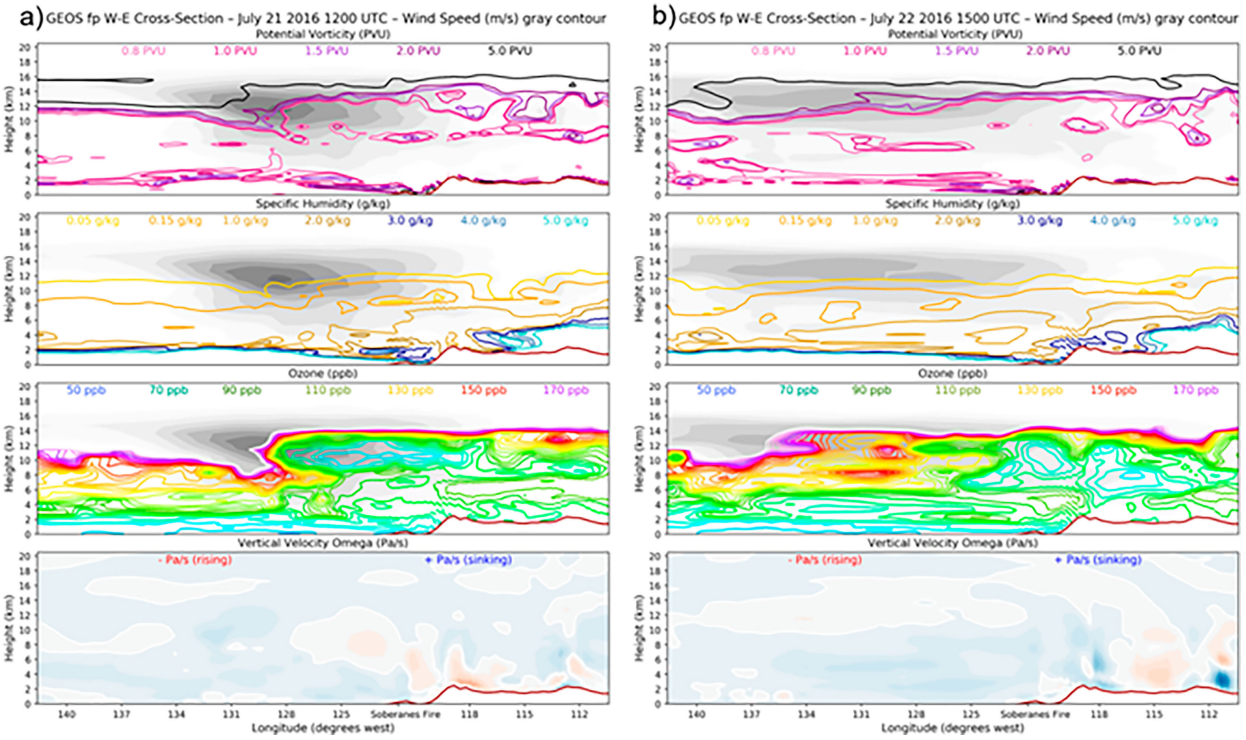

FIG. 5. As in Fig. 4, but for the west–east cross section (magenta line in Fig. 3).

the eastern North Pacific Ocean, along with another broad ridge of high pressure over the desert southwest (Fig. 3, top left). Extending westward from the broad upper-level trough is a large upper-level enclosed low pressure system. The upper-level enclosed low cuts off from the jet stream and progresses westerly out of the domain with time, thus creating multiple embedded shortwave troughs that progress upstream (Fig. 3, top left). At the back-trajectory start time, two centers

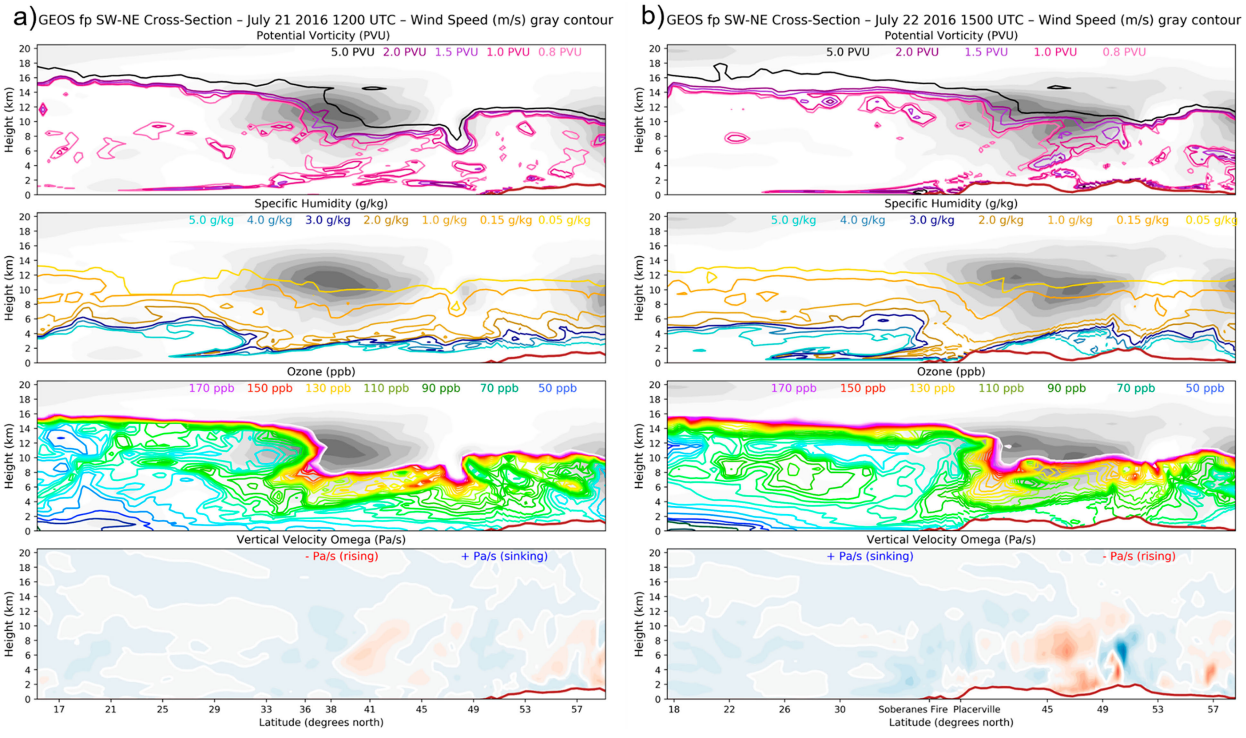

FIG. 6. As in Fig. 4, but for the southwest–northeast cross section (green line in Fig. 3).

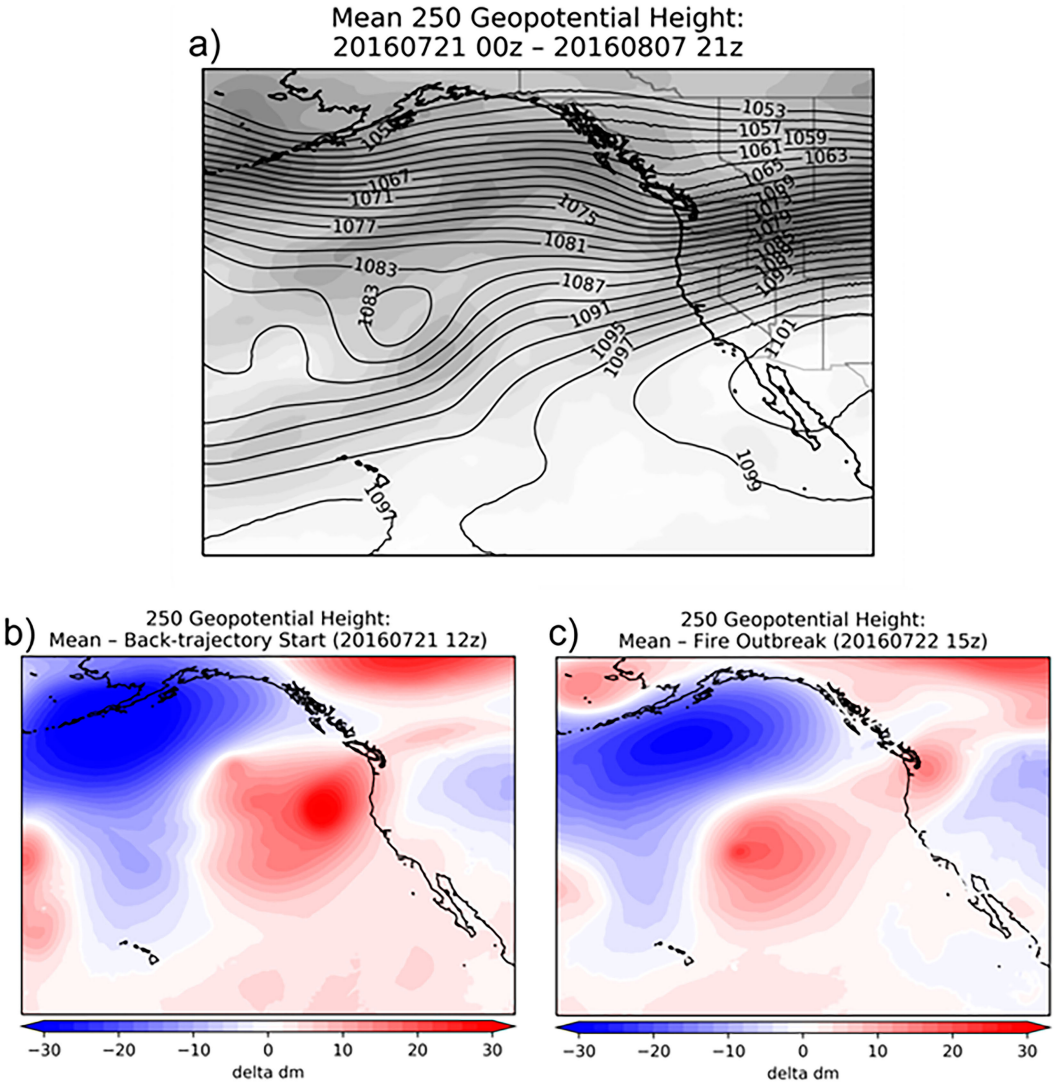

FIG. 7. GEOS-FP 250-hPa geopotential height: (a) average for period 0000 UTC 21 Jul–2100 UTC 7 Aug 2016 (gray shades represent the jet stream), (b) average for back-trajectory start at 1200 UTC 21 Jul 2016, and (c) average for Soberanes Fire outbreak at 1500 UTC 22 Jul 2016.

of enclosed lows are present along the broad and deep trough dominant in the Gulf of Alaska.

Over the next 27 h (1500 UTC 22 July), the upper-level low centers pull apart (Fig. 3, bottom left). Notice that at the time of back-trajectory arrival the eastern center of low pressure lifts and progresses along the jet stream, reaching the Pacific Northwest (PNW) and British Columbia, Canada (BC), coastline. The western low extends southwesterly and develops, deepening and continuing the pattern of a diverging jet stream over the ocean, and the polar jet along the Alaskan coastline strengthens with time as higher pressure builds easterly into the Gulf of Alaska. Note the presence of the zonal flow of the polar jet across North America and the zonal flow of the subtropical jet across the U.S.–Canada border atop a broad ridge of high pressure over southern North America (Fig. 3, left column). Over the eastern North Pacific, the broad, deep trough diverges from the polar jet south to converge with the subtropical jet as the upper-level enclosed low progresses to the shoreline. The broad subtropical jet extended from Canada to the central coast of California, where the Soberanes Fire ignited.

The 700-hPa California mesoscale domain shows at back-trajectory start time, the rising motion is dominant over most of California and the northwest coast. At this low-troposphere level, a dominant weak sinking motion is present offshore of the Soberanes Fire site at the start point. Figure 3 (right column), which suggests a disorganized low-level frontal system offshore approaching the coastline. There is a dominant southerly flow along the coastline and over the land. Offshore from the Soberanes Fire, a dominant southwesterly to westerly flow

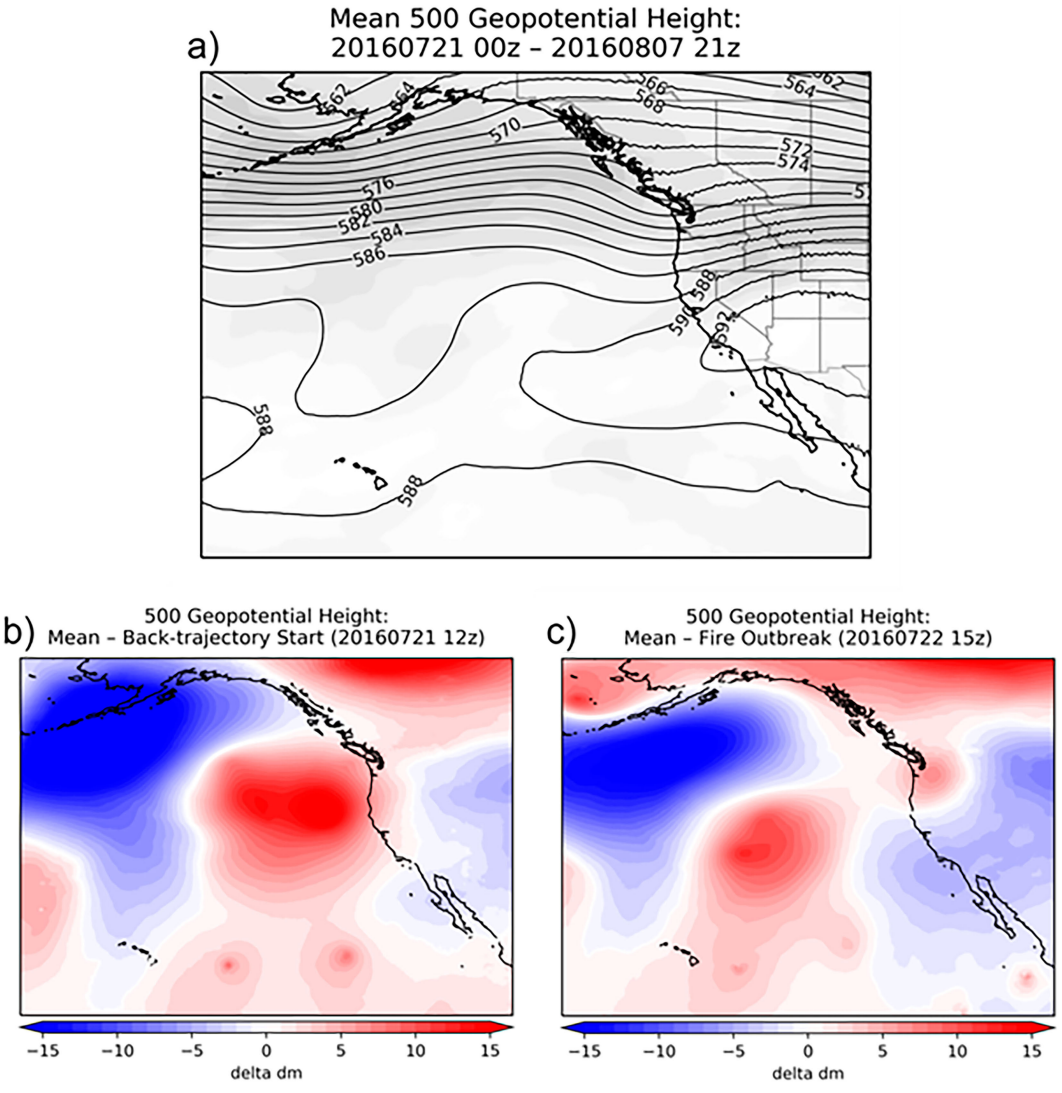

FIG. 8. As in Fig. 7, but for 500-hPa geopotential height.

can be seen in the southern domain. The Soberanes Fire is marked with a pink star (Fig. 3, right column).

Over the next 27 h, the winds aloft the Soberanes Fire decrease in speed and shift from south-southwesterly to westerly (Fig. 3, bottom right). The wind shift represents a frontal passing and the building of high pressure in the southern part of the domain. At the back-trajectory arrival, the sinking motion has moved in across most of the domain and strengthened in the central coastal California region, including the Soberanes Fire ignition point. The cross section along the HYSPLIT back-trajectory path will evaluate the approaching and lifting of the southern end of an SI event across a northeasterly moving jet stream as the dry air entering the lower 500–1250 m AGL enters from the west.

c. *Multiple-cross-sectional analysis*

All of the cross sections presented in this study evaluated a large cross section along the midlatitudes to fully gauge the scale of the deep offshore SI event and the placement of the jet maximums important to the occurrence of a tropopause fold. Figure 3 shows the position of the upper-level trough with the digging enclosed low pressure system places a convergent zone slightly northwest of the cross section intersect at 1200 UTC 21 July. By 1500 UTC 22 July, the area of upper-level convergence has progressed eastward but remains to have a positive tilted axis. Figures 4–6 present the data for the time and location of the lines in Fig. 3. Corresponding to the start time of the model back-trajectories, the left panels of the three cross sections intersect at the starting point. The right panels of Figs. 4–6 intersect at the Soberanes Fire ignition point during the minutes following the outbreak.

For each of the three cross sections at the back-trajectory start time of 1200 UTC 21 July, the subtropical jet stream is aloft at the start point of 128°W and 36°–38°N (Figs. 4a, 5a, and 6a). By the time of the Soberanes Fire outbreak at 1500 UTC 22 July, the subtropical jet stream has shifted to the east and northward (Fig. 3). The green cross sections outlined in Fig. 3

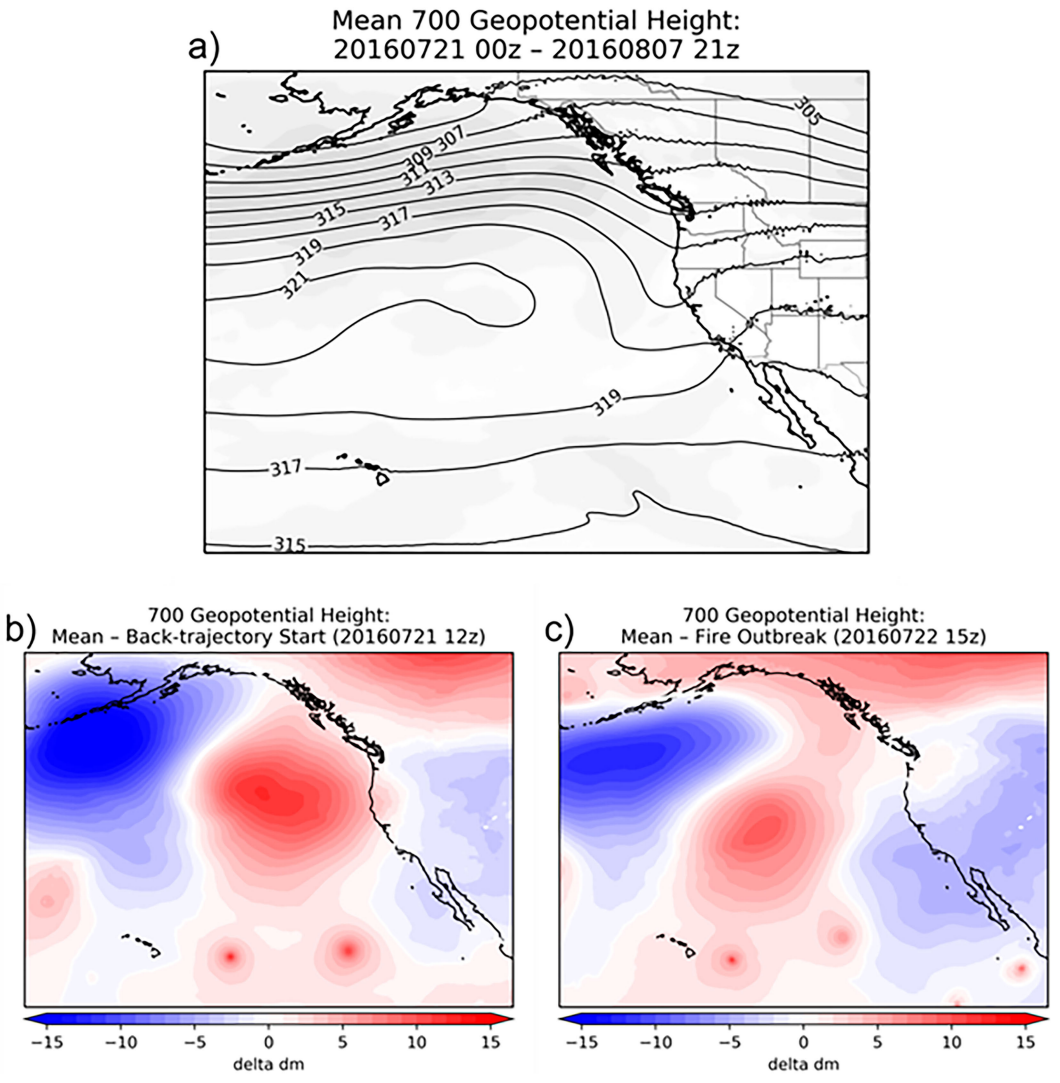

FIG. 9. As in Fig. 7, but for 700-hPa geopotential height.

and presented in Fig. 6 continue to illustrate a slice through the upper-level convergence zone, with upper-level convergence partnering with sinking air and low-level diffluence, allowing for the transport of stratospheric air into the troposphere. This result was consistent with a classic representation of the dry intrusions flow studied by Danielsen et al. (1987) and Browning (1997) that shows that the back-trajectories that are above the surface high pressure behind the upper-level directional flow extend to lower heights of the troposphere. The southwest–northeast cross sections in Fig. 6 therefore allow us to evaluate the progression of the convergence zone as this feature stays centered as the evaluated cross section shifts eastward and takes a stronger northeasterly direction as the embedded upper-level lows shown in Fig. 3 diverge. The northwest–southeast blue cross sections outlined in Fig. 3 and presented in Fig. 4 show us the strengthening of jet to the northwest of the deep trough and a weakening of the jet to the southeast as the embedded enclosed upper-level lows diverge.

The multiple cross-section analysis depicts the presence of a deep offshore SI event around 120°W and between 36° and 38°N, the start point. Along both the northwest–southeast and southwest–northeast cross sections, there is near total column positive omega, indicating sinking motion (Figs. 4a and 6a). This is set between the jet maxima of the upper-level enclosed low. The GEOS-FP modeled PV, SH, and O_3 each demonstrate tropopause folds, injecting higher PVU, rich dry-O_3 stratospheric air southward into the lower 2–4 km of the atmosphere. The west–east cross section shows that this low-level air mass is associated with low-level sinking motion (Fig. 5a).

Figure 5b clearly shows the westward push of the sinking motion. Moving onshore and to the time of the Soberanes Fire outbreak, the multiple cross-sectional analysis indicates the transport of the dry stratospheric air to the coastal Soberanes Fire site and to the lowest 2 km of the troposphere (Figs. 4b, 5b, and 6b). The cross-section evaluation suggests that the critically dry air that was transported to the Soberanes Fire ignition site

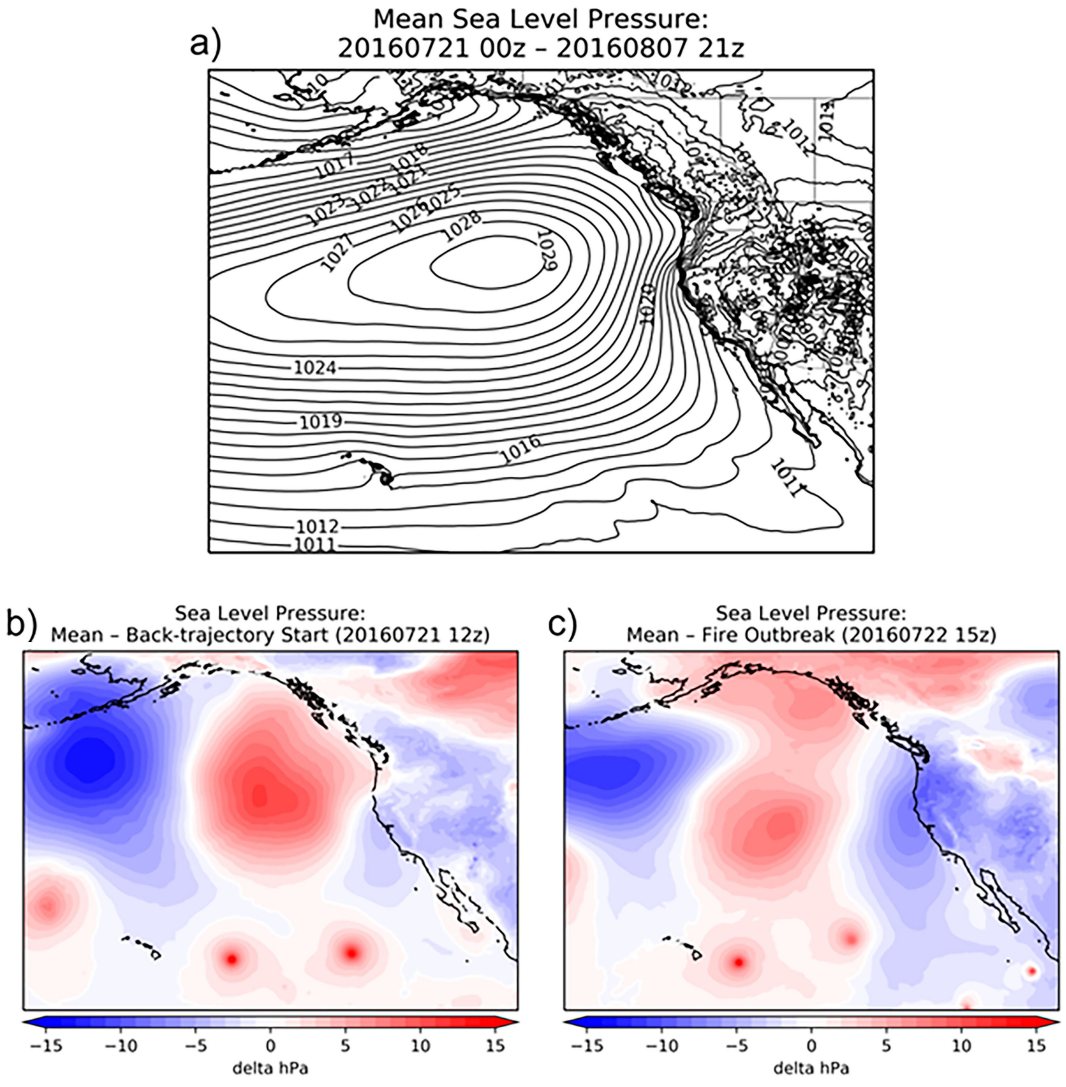

FIG. 10. As in Fig. 7, but for sea level pressure.

on the morning of the outbreak was from a deep offshore SI event that enhanced the fire weather conditions along the central California coastline.

d. Soberanes Fire stage-1 analysis: Period averages and anomalies

As discussed in section 2, stage 1 of Soberanes Fire represents the period from 0000 UTC 21 July through 2100 UTC 7 August. Around the tropopause, as shown in Fig. 7a, the average 250-hPa geopotential heights showed diverging winds over the Pacific Ocean with an enclosed upper-level low west of California, north of the Hawaiian Islands, and south of Alaska. Winds converged at the western U.S. coastline with a weak low pressure trough at the BC–PNW coast and a broad ridge of high pressure aloft in the desert southwest, with the highest pressure across Baja California, Arizona, and New Mexico. Also, the average indicates a zonal jet maximum that extended across the PNW. It appears that the convergent upper-level winds averaged during the first stage of the Soberanes Fire by 7 August 2016 are a sign for prevailing subsidence in the upper troposphere during this period over the region.

The 250-hPa geopotential height anomalies indicate a broadening of the higher pressure ridge aloft in the desert Southwest westward toward the southwest coastline of the North American continents as blue replaces red (Figs. 7b,c). The anomalies also show the development of the two embedded low pressure systems pulling apart with time and causing the lower pressure trough to have a positive tilt and strengthen. In the southern region of the domain, a few weak upper-level low centers progress westward along the tropics.

The average 500-hPa geopotential heights also indicate a low pressure trough in the open Pacific Ocean near the islands of Hawaii; showing a closed subtropical high aloft located over the desert Southwest and the belt of westerlies to the north (Fig. 8a). The average 500-hPa geopotential heights

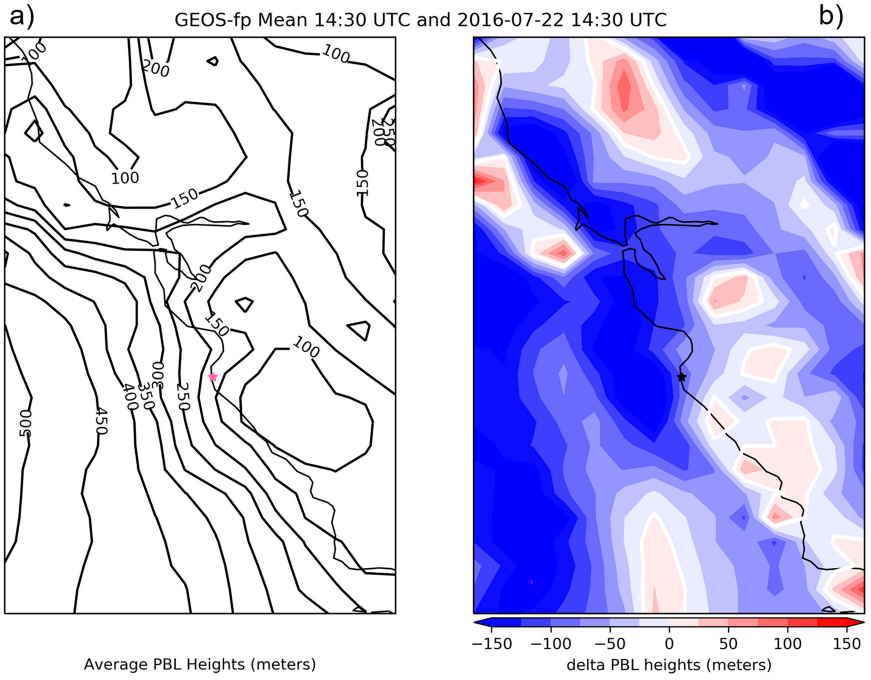

FIG. 11. GEOS-FP PBL heights for (a) the period average at 1430 UTC (the pink star marks the coastal ignition point) and (b) the period average minus the fire-outbreak date (the black star marks the coastal ignition point).

pattern produces summertime heatwaves in California and is indicative of the subtropical-high-aloft pattern, which brings critical fire weather to the western U.S. states and is of greater importance to California (Schroeder 1969). Note, from the average, a shortwave trough at the coastline. This bears an even stronger presence at 700 hPa (Fig. 9a).

At 500 hPa, the geopotential height anomalies again indicate the separation of two enclosed centers of low pressure,

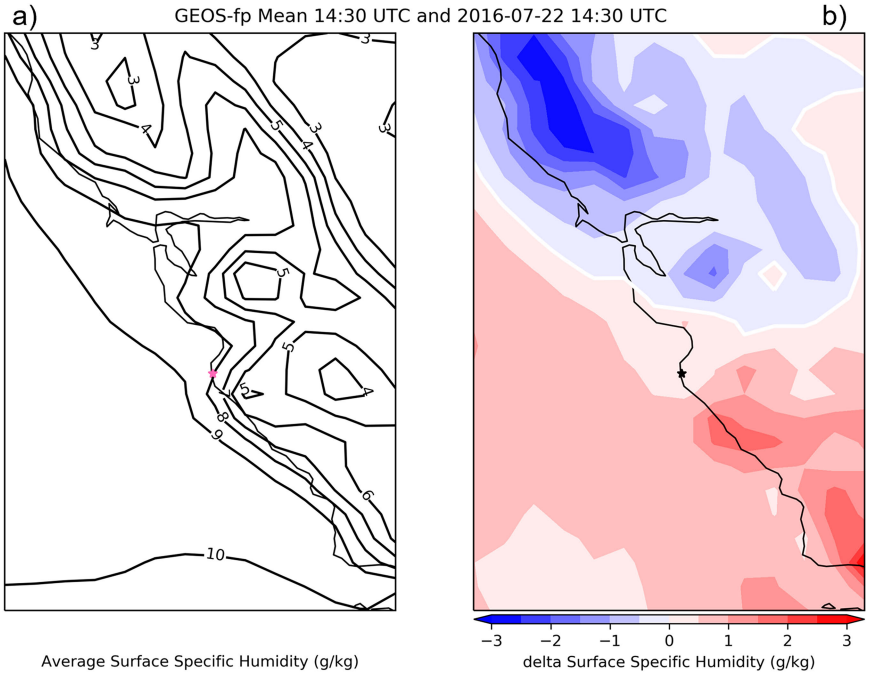

FIG. 12. As in Fig. 11, but for surface specific humidity.

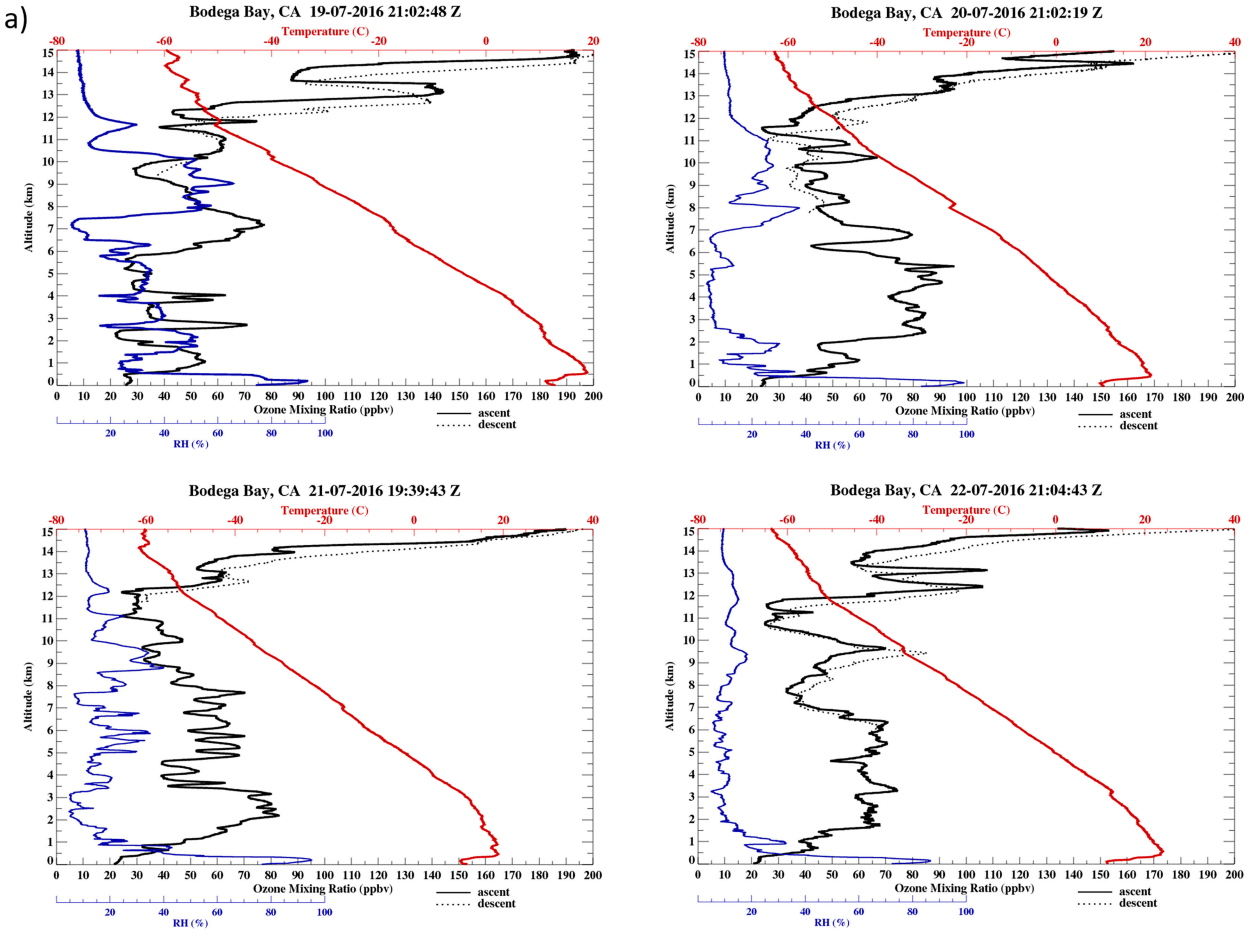

FIG. 13. Bodega Bay (a) O_3, relative humidity, and temperature and (b) wind vertical profiles from 19 to 22 Jul 2016 (CABOTS-SJSU 2016).

one that progresses westward over Washington State and one that digs to the southeast (Figs. 8b,c). The building of higher pressure is recognizable aloft over western North America and offshore of California. The development of the low pressure centers along the tropics is even clearer.

A noticeable feature in Fig. 9a is that the average 700-hPa geopotential heights indicate a trough along the coastline dipping down into southern California , signs of frontal passings. An important observation of Fox-Hughes (2015) while studying "spike" days with elevated chances of extreme fire behavior in Tasmania was the presence of a cold front. The fronts were embedded in a broad trough and were either approaching or recently crossed the state. In the current study the greatest 700-hPa heights are over a broad region west of California with the low-level jet in the Gulf of Alaska set atop the area of higher pressure. Equatorward, wiggles in the 315-dam (dekameter) contour are a clear sign of tropical depressions.

The depth of the upper-level low pressure system is recognizable in the 700-hPa height anomalies (Figs. 9b,c). Again, the building of higher pressure centered over Baja California is clear along with the development of tropical cyclones during that time. During the evaluation period, six eastern Pacific tropical depressions were present. Notice the waves in the isobars from 1011 to 1015 hPa along the coast of Mexico and along the tropics to Hawaii shown in the average sea level pressure (SLP; Fig. 10a). These isobars also bend to be north–south along the California coastline. During this period, the average SLP shows a dominant area of high pressure triangulated between the Aleutian and Hawaiians Islands and the PNW, indicating the ever-so-common presence of the Pacific high (Fig. 10a).

The SLP anomalies indicated high pressure building along the North America coastline (Figs. 10b and 9c). Two more eastern Pacific tropical depressions formed off the Mexican coast by 1500 UTC 22 July, and the initial two have moved westward toward the Hawaiian Islands (Fig. 10c).

All levels evaluated indicate a westward shift of offshore lower pressure (i.e., reds in Figs. 10b,c). The upper levels of the atmosphere show the presence of an upper-level shortwave trough that digs and strengthens into a cutoff low and retrogrades while another enclosed upper-level low weakens and progresses upstream. In the lower levels of the atmosphere, multiple low-level tropical cyclones continue on their westward track and two more develop off the shores of Baja California. The overall picture indicates the building of higher pressure (blues in Figs. 10b,c) over the continental west as the Soberanes Fire outbreak occurs and, therefore, a strengthening

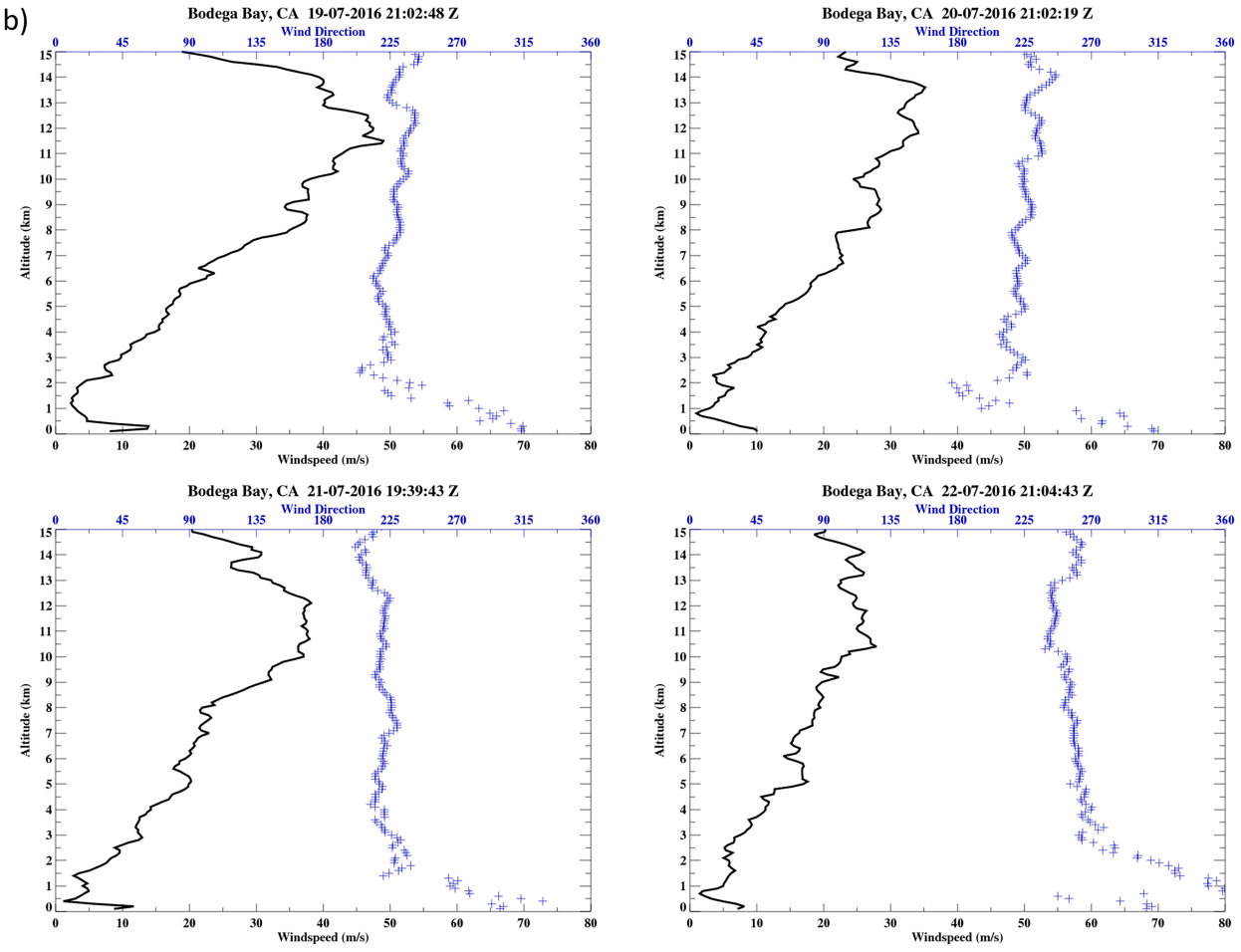

FIG. 13. *(Continued)*.

of the subtropical high aloft. It is a key component to critical fire weather across California. The building of the high pressure with time may play a role to assist in the continued descent of the stratospheric air injection from the 700-hPa level to the lowest 1.25 km above the Soberanes Fire during ignition.

e. Local PBL heights and surface specific humidity

The period average of 1430 UTC indicates relatively low PBL heights in the region over land and the steepest gradient offshore (Fig. 11a). Average morning PBL heights at the Soberanes Fire is between 150 and 200 m high. On the morning of the Soberanes Fire outbreak, PBL heights were higher than the period average across much of the local region (Fig. 11b). At the Soberanes Fire, the model data indicate PBL heights were 75–100 m higher than the average. Furthermore, the back-trajectory analysis suggested that the very dry air descended to about 250 m AGL, which would enhance the dry condition near the surface in the area of the fire outbreak.

The period average 1430 UTC surface SH values indicate that the driest areas were located in the California valleys, increasing in humidity outward from these zones and offshore (Fig. 12a). At the fire site (pink star), this value was around 8 g kg^{-1}. On the morning of the fire outbreak, the moister air was in the northern portion of the domain and heavily along the northern coastal mountains (Fig. 12b). The southern half of the domain and offshore exhibited conditions above the period average and were, therefore, drier at the time of the Soberanes Fire outbreak. At the Soberanes Fire site, the air was about 0.5 g kg^{-1} drier than the period average (Fig. 12b, black star).

f. Observational findings during CABOTS 2016

The California Baseline Ozone Transport Study (CABOTS) was conducted from May to August 2016 (Faloona et al. 2020) during which a near-daily ozonesonde was launched from Bodega Bay (BBY), California. Surface observations at the time of launch, a descriptive forecast for upcoming days, model and satellite observations, and a vertical profile and path of the ozonesonde were summarized daily. A review of the BBY vertical profiles from 19 to 22 July presented the changes in wind direction, wind speed, O_3 concentrations, and RH values beginning during the offshore SI event through to the afternoon after the Soberanes Fire outbreak

(Fig. 13). First we review the vertical wind profiles in Fig. 13b: on 19 July winds from 3 km up are southwesterly following the flow of the upper-level trough. By 20 July this is true to 2.5 km, and, by 21 July in the afternoon before the fire, southwesterly winds aloft are measured as low as 1.5 km above the surface. By the afternoon of 22 July, the winds aloft shift to west-southwesterly from 3 km up (Fig. 13b). One indication of the deepening influence of the upper levels to the lower levels of the troposphere was the depths to which the winds aloft reach. Correspondingly, the NWS surface observations show the placement of an upper-level trough above the Soberanes Fire locale that was present from 0900 until 2100 UTC 22 July (not shown).

Along with the wind direction, the drying of the vertical column occurs (Fig. 13a). On 19 July, from the surface to 7 km, there were layers of drier air with 20% RH or less that correspond to elevated layers of O_3. On 20 July between 2.5 and 5.5 km, there was a definitive thick layer of very dry air with ~5% RH and elevated O_3 values ranging from 70 to 100 ppb, the greatest values observed in the tropospheric column. Also, there was a thin layer present near 1 km with O_3 peaking at 60 ppb and RH $< 10\%$. By 2030 UTC 20 July, the GEOS-West water vapor imagery clearly depicts a "dry slot": a dark band over the eastern Pacific Ocean and swooping northeasterly across the California coast that remains present at 1930 UTC 21 July (Fig. 14). The presence of dry bands typically results in abrupt surface drying and gusty winds (e.g., Schoeffler 2009). From Fig. 13a, the 21 July vertical profiles showed the driest air of ~5% RH was at 2–3 km and was associated with O_3 values of ~80 ppm. By 22 July, above the marine BL around 0.5 km, the vertical column was well below 20% RH except near 1 km and O_3 was near 65 ppb from 1.5 to 6.5 km.

In addition, a review of the Chews Ridge, California, surface observations indicates the arrival of dry, warm, gusty air to the local fire region (e.g., Potter 2016). The Chews Ridge surface station is elevated near 1.5 km above mean sea level (MSL) and is located to the southeast of the Soberanes Fire and the BBY ozonesonde launch site. Of the available CABOTS data, this set is in close proximity to the Soberanes Fire and was therefore chosen; the fire eventually reaches and burns through Chews Ridge, California. The surface observations from 1100 PST (1800 UTC) 19 July through 2300 PST 22 July showed an overall warming and drying trend with time and an increase in wind speed corresponding to a westerly turn in the winds (Fig. 15). At the beginning of the period, RH values approached 50%, and they decreased to ~5% on 2000 PST 22 July. Critical values below 20% were continuously observed starting at 0800 PST (1500 UTC) 21 July and through 1500 PST (2200 UTC) 22 July, coinciding with the strongest wind speeds of the period and the dominant westerly–west-southwesterly directions. Two hours prior to the Soberanes Fire outbreak, wind speed hit the period maximum of 14 mi h^{-1} (6.3 m s^{-1}): 4 times that of the period average wind speed. Linking up with the time of the Soberanes Fire outbreak, at 0800 PST (1500 UTC) 22 July, RH dropped down to only 7%. The winds remained westerly since the previous day.

Together, these meteorological observations at BBY and Chews Ridge and the GOES-West satellite water vapor imagery support the presence of the identified SI event leading up to the Soberanes Fire outbreak.

4. Conclusions and remarks

This study investigated the synoptic setup and mesoscale transport of a deep SI event that brought extreme fire weather conditions to the coastal mountains where the Soberanes Fire ignited, indicating a connection between the events. From this analysis, we can conclude a connection between an offshore SI event and the Soberanes Fire outbreak. At 1200 UTC 21 July 2016, the GEOS-FP model results of 250-hPa geopotential height and multiple-cross-sectional analysis of PV, SH, O_3, and omega demonstrate the presence of an offshore deep dry stratospheric air intrusion. The NOAA HYSPLIT model back-trajectory analysis shows the driest air descended to the lowest 1.25 km aloft the Soberanes Fire from near 36°–38°N, 128°W and starting above 2.5 km, the location and timing of the identified offshore deep SI event. At 1500 UTC 22 July, the multiple-cross-sectional analysis suggests the northwesterly progression of the SI event and the westerly low-level descent and transport of the dry stratospheric air down constant isentropes along the back-trajectory path to the Soberanes Fire.

The period average analysis strengthened the connection between the SI occurrence and the arrival of dangerous fire conditions. The synoptic analysis allowed us to understand the atmospheric setup for the Rossby wave break, which adds to the complexity of the stratospheric dry air transport down into the troposphere, including a remote influence over the location of the Soberanes Fire development as well as the westward push of sinking motion while the main push of sinking motion is coming from the north, related directly to the upper-level PV anomaly. Furthermore, the mesoscale analysis indicates the continued transport inland to the coastal Soberanes Fire. A building of high pressure at the surface and at 700 hPa contributed to the continued descent and drying of the low-level stratospheric air reaching the lowest 1.25 km aloft of the Soberanes Fire. The local region analysis of the morning (i.e., 1430 UTC) averages show that just before the Soberanes Fire outbreak on 22 July the PBL heights were above the period average and the surface SH values were drier. Together with the HYSPLIT back-trajectory analysis, it can be inferred that some of the transported dry stratospheric air likely entered into the surrounding elevated PBL heights in the local Soberanes Fire area.

From this study, it can be concluded that offshore deep SI events can aid in transporting extremely dry air to the western California coastline, therefore aiding conditions of extreme fire weather. Although not shown, a back-trajectory and cross-sectional analysis suggest similar conditions leading up to the Los Angeles County Sand Fire, which ignited a few hours after the Soberanes Fire at 2000 UTC 22 July 2016. Also, this method for a period of accelerated Soberanes Fire growth overnight of 3–4 August 2016 indicates a low-level dispersion of stratospheric air likely transported to the region after a quick progression of an upper-level enclosed low as it

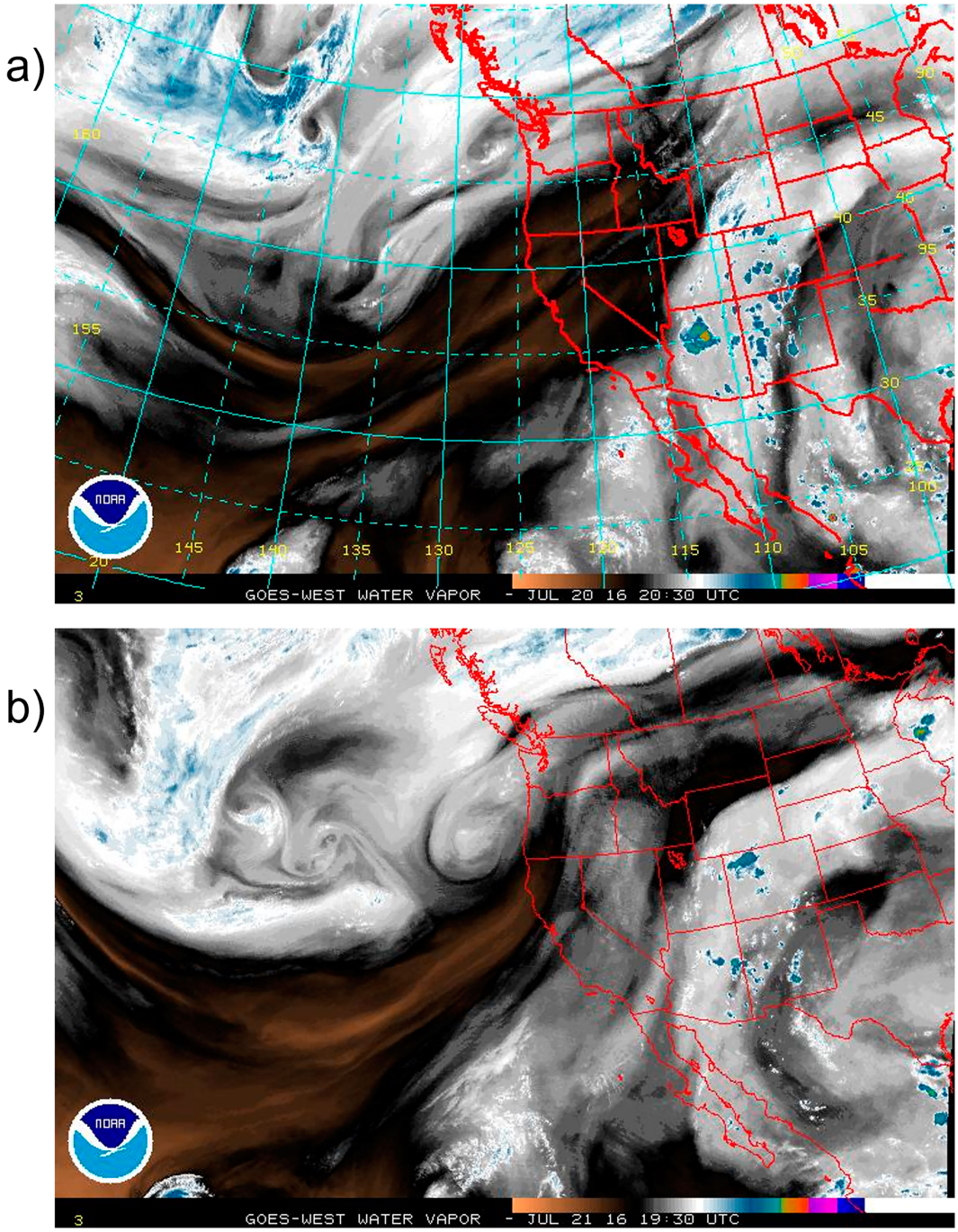

FIG. 14. GOES-West water vapor imagery from (a) 2030 UTC 20 and (b) 1930 UTC 21 Jul 2016.

approached and crossed the BC–PNW coastline and the associated tropopause Rossby wave breaks.

During the time of the Soberanes Fire, the Pacific–North American teleconnection pattern (PNA) is at its weakest and is dominated by cyclones, the hurricane season associated with tropical upper-tropospheric trough (TUTT) has begun, and the North American monsoon is in action, with all of these processes potentially aiding in the westward transport of a deep offshore stratospheric dry air intrusion to the western United States. The prediction of low-level transport of dry stratospheric air to the coastal communities could help to predict the occurrence of wildfire outbreaks or of periods of accelerated fire growth. This would be a useful tool for fire districts and air quality districts. All of this leads to a need to study further the influence of dry stratospheric air transport on western coastal fires during the wildfire season of July and

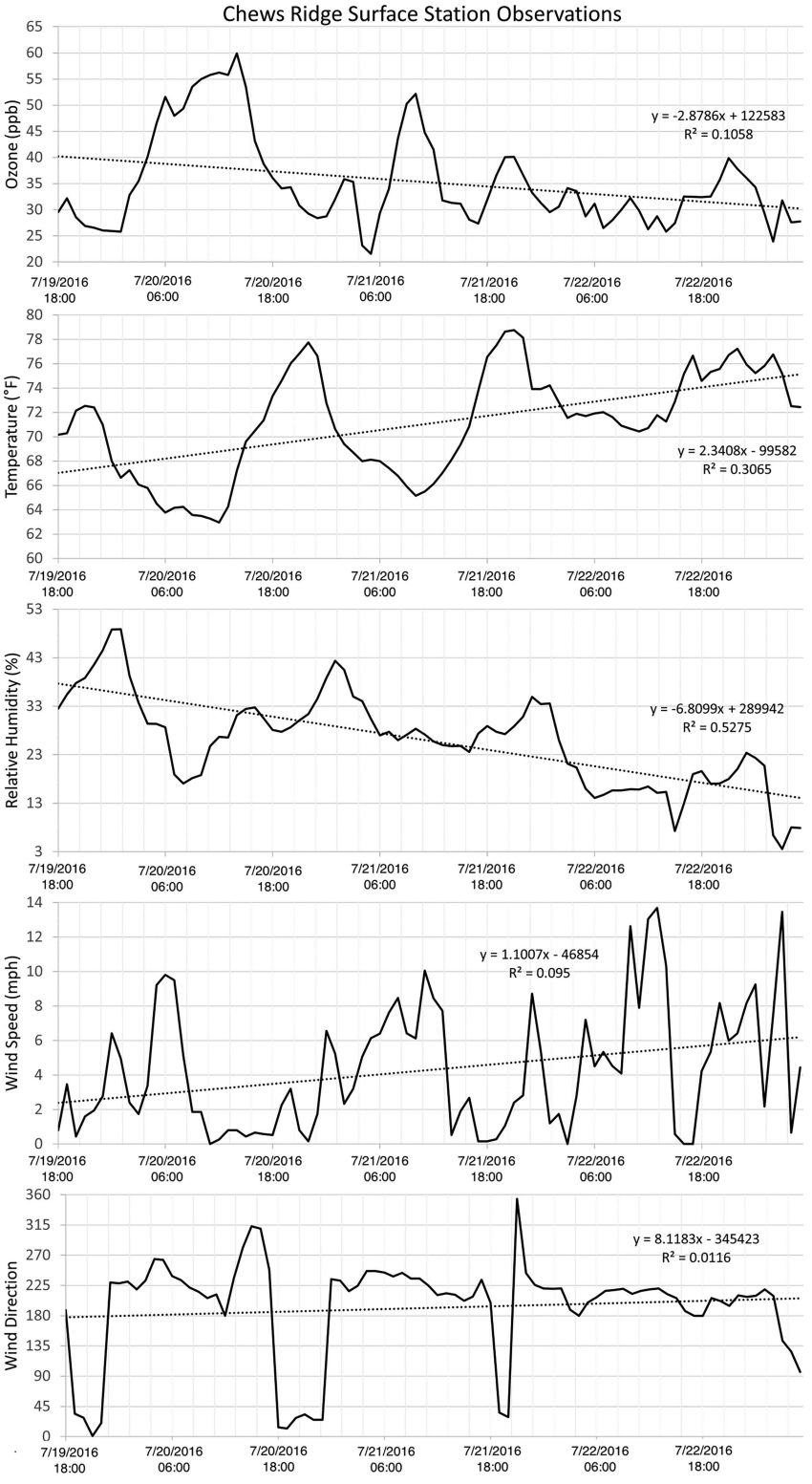

FIG. 15. Time evolution (horizontal axis; UTC) of surface observations (ozone, temperature, RH, wind speed, and direction) at Chews Ridge during CABOTS 2016.

August. This method could potentially serve other Mediterranean climate regions globally that are also SI event hotspots. As our climate continues to evolve with global warming, it is imperative to investigate further the evolution of stratospheric air transport across multiple scales and all impacts of its transport, including pollution and dangers from O_3 and wildfire.

Acknowledgments. We acknowledge the suppliers of datasets utilized in this research. Comments and suggestions by three anonymous reviewers were much appreciated. This study was supported by the NOAA Educational Partnership Program with Minority-Serving Institutions Cooperative Agreement NA22SEC4810015.

Data availability statement. The data (GEOS-FP, HYSPLIT) described in this paper are publicly available. Python scripts for processing data in this paper are available upon request.

REFERENCES

Boegelsack, N., J. Withey, G. O'Sullivan, and D. McMartin, 2018: A critical examination of the relationship between wildfires and climate change with consideration of the human impact. *J. Environ. Prot.*, **9**, 461–467, https://doi.org/10.4236/jep.2018.95028.

Browning, K. A., 1997: The dry intrusion perspective of extratropical cyclone development. *Meteor. Appl.*, **4**, 317–324, https://doi.org/10.1017/S1350482797000613.

CABOTS-SJSU, 2016: Bodega Bay ozonesonde launch blog. Accessed 1 June 2023, https://sites.google.com/a/sjsu.edu/cabots-sjsu/launch-blog-bodega-bay.

Cho, J. Y. N., R. E. Newell, E. V. Browell, W. B. Grant, C. F. Butler, and M. A. Fen, 2001: Observation of pollution plume capping by a tropopause fold. *Geophys. Res. Lett.*, **28**, 3243–3246, https://doi.org/10.1029/2001GL012898.

Clark, J., and S. Chiao, 2019: A case study of stratospheric ozone transport to the northern San Francisco Bay area and Sacramento valley during CABOTS 2016. *J. Appl. Meteor. Climatol.*, **58**, 2675–2697, https://doi.org/10.1175/JAMC-D-18-0322.1.

Cox, B. D., M. Bithell, and L. J. Gray, 1997: Modelling of stratospheric intrusions within a mid-latitude synoptic-scale disturbance. *Quart. J. Roy. Meteor. Soc.*, **123**, 1377–1403, https://doi.org/10.1002/qj.49712354112.

Danielsen, E. F., R. S. Hipskind, S. E. Gaines, G. W. Sachse, G. L. Gregory, and G. F. Hill, 1987: Three-dimensional analysis of potential vorticity associated with tropopause folds and observed variations of ozone and carbon monoxide. *J. Geophys. Res.*, **92**, 2103–2111, https://doi.org/10.1029/JD092iD02p02103.

Faloona, I. C., and Coauthors, 2020: The California Baseline Ozone Transport Study (CABOTS). *Bull. Amer. Meteor. Soc.*, **101**, E427–E445, https://doi.org/10.1175/BAMS-D-18-0302.1.

Fox-Hughes, P., 2015: Characteristics of some days involving abrupt increases in fire danger. *J. Appl. Meteor. Climatol.*, **54**, 2353–2363, https://doi.org/10.1175/JAMC-D-15-0062.1.

Funatsu, B. M., and D. W. Waugh, 2008: Connections between potential vorticity intrusions and convection in the eastern tropical Pacific. *J. Atmos. Sci.*, **65**, 987–1002, https://doi.org/10.1175/2007JAS2248.1.

Georgiev, C. G., S. A. Tjemkes, A. Karagiannidis, J. Prieto, and K. Lagouvardos, 2022: Observational analyses of dry intrusions and increased ozone concentrations in the environment of wildfires. *Atmosphere*, **13**, 597, https://doi.org/10.3390/atmos13040597.

Langford, A. O., R. B. Pierce, and P. J. Schultz, 2015: Stratospheric intrusions, the Santa Ana winds, and wildland fires in Southern California. *Geophys. Res. Lett.*, **42**, 6091–6097, https://doi.org/10.1002/2015GL064964.

Mass, C. F., and D. Ovens, 2019: The Northern California wildfires of 8–9 October 2017: The role of a major downslope wind event. *Bull. Amer. Meteor. Soc.*, **100**, 235–256, https://doi.org/10.1175/BAMS-D-18-0037.1.

Mills, G., 2008: Abrupt surface drying and fire weather Part 1: Overview and case study of the South Australian fires of 11 January 2005. *Aust. Meteor. Mag.*, **57**, 299–309.

Oltmans, S. J., and Coauthors, 2010: Enhanced ozone over western North America from biomass burning in Eurasia during April 2008 as seen in surface and profile observations. *Atmos. Environ.*, **44**, 4497–4509, https://doi.org/10.1016/j.atmosenv.2010.07.004.

Potter, C., 2016: Landscape patterns of burn severity in the Soberanes Fire of 2016. *J. Geogr. Nat. Disasters*, **S6**, 005, https://doi.org/10.4172/2167-0587.S6-005.

Roelofs, G. J., and Coauthors, 2003: Intercomparison of tropospheric ozone models: Ozone transport in a complex tropopause folding event. *J. Geophys. Res.*, **108**, 8529, https://doi.org/10.1029/2003JD003462.

Schoeffler, F. J., 2009: Large wildfire growth influenced by tropospheric and stratospheric dry slots in the United States. *Proc. 17th Conf. on Atmospheric and Oceanic Fluid Dynamics*, Newport, RI, Amer. Meteor. Soc., 5.1, https://ams.confex.com/ams/19Fluid17Middle/webprogram/Handout/Paper225271/EDITTING%20AMS%20FINAL%20Large%20Wildfire%20Growth%20Influenced%20By%20Tropospheric%20and%20Stratospheric%20Dry%20Slots%20In%20The%20U.S..pdf.

Schroeder, M. J., 1969: Critical fire weather patterns in the conterminous United States. ESSA Tech. Rep. WB 8, 31 pp.

Škerlak, B., M. Sprenger, and H. Wernli, 2014: A global climatology of stratosphere–troposphere exchange using the ERA-Interim data set from 1979 to 2011. *Atmos. Chem. Phys.*, **14**, 913–937, https://doi.org/10.5194/acp-14-913-2014.

Spracklen, D. V., L. J. Mickley, J. A. Logan, R. C. Hudman, R. Yevich, M. D. Flannigan, and A. L. Westerling, 2009: Impacts of climate change from 2000 to 2050 on wildfire activity and carbonaceous aerosol concentrations in the western United States. *J. Geophys. Res.*, **114**, D20301, https://doi.org/10.1029/2008JD010966.

Stein, A. F., R. R. Draxler, G. D. Rolph, B. J. B. Stunder, M. D. Cohen, and F. Ngan, 2015: NOAA's HYSPLIT atmospheric transport and dispersion modeling system. *Bull. Amer. Meteor. Soc.*, **96**, 2059–2077, https://doi.org/10.1175/BAMS-D-14-00110.1.

Trickl, T., H. Vogelmann, H. Giehl, H.-E. Scheel, M. Sprenger, and A. Stohl, 2014: How stratospheric are deep stratospheric intrusions? *Atmos. Chem. Phys.*, **14**, 9941–9961, https://doi.org/10.5194/acp-14-9941-2014.

Werth, P. A., and Coauthors, 2011: Synthesis of knowledge of extreme fire behavior: Volume 1 for fire managers. General Tech. Rep. PNW-GTR-854, 144 pp., https://doi.org/10.2737/PNW-GTR-854.

Williams, A. P., J. T. Abatzoglou, A. Gershunov, J. Guzman-Morales, D. A. Bishop, J. K. Balch, and D. P. Lettenmaier,

2019: Observed impacts of anthropogenic climate change on wildfire in California. *Earth's Future*, **7**, 892–910, https://doi.org/10.1029/2019EF001210.

Zhong, S., L. Yu, W. E. Heilman, X. Bian, and H. Fromm, 2020: Synoptic weather patterns for large wildfires in the northwestern United States—A climatological analysis using three classification methods. *Theor. Appl. Climatol.*, **141**, 1057–1073, https://doi.org/10.1007/s00704-020-03235-y.

Zimet, T., J. E. Martin, and B. E. Potter, 2007: The influence of an upper-level frontal zone on the Mack Lake wildfire environment. *Meteor. Appl.*, **14**, 131–147, https://doi.org/10.1002/met.14.